Hydrological Sciences Journal

ISSN: 0262-6667 (Print) 2150-3435 (Online) Journal homepage: www.tandfonline.com/journals/thsj20

Uncertainty propagation from gridded precipitation datasets to streamflow simulations: application to the Reno River basin (Italy)

Omar Cenobio-Cruz & Giuliano Di Baldassarre

HYDROLOGICAL SCIENCES JOURNAL
https://doi.org/10.1080/02626667.2025.2590597

OPEN ACCESS

Uncertainty propagation from gridded precipitation datasets to streamflow simulations: application to the Reno River basin (Italy)

Omar Cenobio-Cruz[a] and Giuliano Di Baldassarre[a,b,c]

[a]Department of Earth Sciences, Uppsala University, Uppsala, Sweden; [b]Department of Earth Sciences, Centre of Natural Hazards and Disaster Science (CNDS), Uppsala University, Uppsala, Sweden; [c]Swedish Centre for Impacts of Climate Extremes (Climes), Uppsala University, Uppsala, Sweden

ABSTRACT
The development of gridded precipitation datasets has accelerated in recent decades, establishing them as crucial tools in hydrological analysis. This study aims to unravel the propagation of uncertainty in hydrological modelling from precipitation data to streamflow simulations. To this end, we examined the impact of using state-of-the-art datasets as model input for the Reno River basin in Italy. Our results show that (1) while seasonal precipitation patterns are similar, wet season and annual averages differ, particularly in the mountainous sub-basin; (2) the mountainous sub-basin exhibits large variability, with winter peak flows frequently underestimated; (3) uncertainties in precipitation propagate into the dry season, where variability is relatively greater than for the entire basin. We also examined the significance of addressing uncertainty in hydrological modelling at various scales. These findings underscore the influence of precipitation data uncertainty on hydrological calculations, particularly in regions with complex topography.

ARTICLE HISTORY
Received 1 July 2025
Accepted 24 October 2025

EDITOR
A. Fiori

ASSOCIATE EDITOR
G. Mascaro

KEYWORDS
Uncertainty propagation; gridded precipitation; hydrological modelling; Italy

1 Introduction

Hydrological modelling has become a tool that provides critical insights for planning and managing water resources (Clark *et al.* 2017). It gives us important information to understand the dynamics of the hydrological cycle (Singh 2018), and supports decision-making processes (e.g. Beven 2012, Vörösmarty *et al.* 2015, Döll *et al.* 2016, Tran *et al.* 2024) and follow-up of natural hazards (e.g. Yuan *et al.* 2015, Clark *et al.* 2017, Tsering *et al.* 2022). Its relevance has grown significantly in light of increasing water demands and the impacts of climate change (Bates *et al.* 2008, Wanders and Wada 2015).

However, hydrological models are inherently affected by different uncertainty sources, which can substantially influence the accuracy of their outcomes (e.g. Di Baldassarre and Montanari 2009, Renard *et al.* 2010, McMillan *et al.* 2012). There are multiple sources of uncertainty, including input data, model structure, and model parameterization (e.g. Moges *et al.* 2021, Gharari *et al.* 2021). Uncertainty in input data, mainly precipitation, is one of the most significant sources (e.g. McMillan *et al.* 2018, Bárdossy *et al.* 2022), as it drives the water cycle and directly influences both the magnitude and timing of runoff (Gupta and Sorooshian 1985, Beven and Binley 1992). Uncertainty related to model structure arises from (unavoidable) assumptions to represent the complexity of hydrological processes (e.g. Montanari and Di Baldassarre 2013, Clark *et al.* 2015, Knoben *et al.* 2020). Parameter uncertainty arises from the fact that most model parameters cannot be directly measured, and that different parameter sets can produce similar hydrological outcomes (e.g. Andréassian *et al.* 2001, Vrugt *et al.* 2003, Engeland *et al.* 2016, Herrera *et al.* 2022).

Precipitation is the main driver of hydrological responses and it exhibits considerable variability worldwide. Thus, it represents a large source of uncertainty that challenges hydrological modelling (e.g. Kidd and Huffman 2011, Sun *et al.* 2018, Mankin *et al.* 2025). Accurate precipitation data is essential for producing reliable hydrological model outcomes (e.g. Pappenberger *et al.* 2011, Tran *et al.* 2024). Recent studies have systematically evaluated the use of gridded precipitation datasets in different regions of Italy. Cavalleri *et al.* (2024) conducted a multi-scale assessment of high-resolution reanalysis precipitation products over Italy. They found spatial biases and systematic differences that should be considered in trend analysis. Alfieri *et al.* (2022) showed that high-resolution satellite-based products in the Po River basin provide a skilful river discharge estimation, supporting the feasibility of fully satellite-driven applications. Similarly, Sarigil *et al.* (2024) forced a rainfall-runoff model with different meteorological products in Northern Italy and found that the dataset selection substantially influences model outputs. Previous research across Italy emphasized the pre-assessment of precipitation datasets in hydrological applications (Camici *et al.* 2018, Gentilucci *et al.* 2022, Longo-Minnolo *et al.* 2022,

CONTACT Omar Cenobio-Cruz omar.cenobio-cruz@geo.uu.se Department of Earth Sciences, Uppsala University, Villavägen 16, Uppsala 75236, Sweden
Supplemental data for this article can be accessed online at https://doi.org/10.1080/02626667.2025.2590597

Cammalleri *et al.* 2024). However, few studies have explicitly investigated how forcing uncertainty propagates into hydrological model outputs in Italy (Nikolopoulos *et al.* 2010, Sarigil *et al.* 2024).

Thus, the quantification of uncertainties in meteorological forcing on hydrological modelling has become a central issue in recent research, particularly when it is used for evaluating water availability and hydrological responses under diverse climatic scenarios (Clark *et al.* 2016). Several studies have highlighted the influence of precipitation uncertainty on streamflow simulations. For instance, Fekete *et al.* (2004) examined the effect of precipitation uncertainty on the global water balance. Their results indicate that uncertainty in runoff is comparable to precipitation uncertainty but particularly large in semi-arid regions. Biemans *et al.* (2009) applied different global precipitation datasets to quantify uncertainty in simulated discharge and demonstrated that uncertainty in discharge is considerably amplified, 3 times higher than uncertainty in precipitation. Another study, by Sperna Weiland *et al.* (2015), using different rainfall data products indicated that precipitation uncertainty remained the main factor affecting simulated discharge accuracy, highlighting the need for a better characterization of precipitation data, especially at finer resolutions. More recently, Tang *et al.* (2025) evaluated the impact of both precipitation and temperature, using an ensemble meteorological dataset, at a global scale, and they found clear uncertainty propagation signals over the different climate regions and areas. Similar efforts to quantify the uncertainty can be found in other recent studies (e.g. Pokorny *et al.* 2020, Schreiner-McGraw and Ajami 2020, 2022, Kabir *et al.* 2022).

Although substantial advances have been made, important research gaps persist. First, the spatial scale of multiple research efforts concentrates on a global scale or continental assessments, neglecting the importance of sub-basin scale variability (Tang *et al.* 2023), which is important for local water resource management. Second, the relation between input data uncertainty and uncertainty in model parameterization – how calibration compensates for input errors – remains not entirely understood (e.g. Fowler *et al.* 2018, Tapas *et al.* 2025). Addressing these gaps is vital to further enhance hydrological simulations, especially for water resources management and climate change (Clark *et al.* 2016, Tran *et al.* 2024). Lastly, although gridded precipitation datasets are increasingly developed and widely used in climate and hydrological studies (e.g. Beck *et al.* 2017b, Tran *et al.* 2023), the impact of their inaccuracies on streamflow simulations remains largely unexplored (Abbas *et al.* 2025).

This study aims to unravel how uncertainty in precipitation data cascades through a process-based hydrological model and influences streamflow predictions. To achieve this, we used the Reno River basin in Italy as a test site and employed different precipitation datasets. First, we quantify uncertainty at seasonal scale, and then evaluate the impacts of this precipitation forcing on the streamflow simulations using the Hydrological Predictions for the Environment (HYPE) model, at both daily and monthly time scales. This study jointly addresses the impact of uncertainty in input precipitation and parameter uncertainty through the application of Monte Carlo simulations for each precipitation dataset.

2 Study area

The Reno River basin extends across the regions of Tuscany and Emilia-Romagna in northern Italy (Fig. 1). The Reno River originates in the Apennine Mountain range and drains into the Adriatic Sea, with an extension of 5040 km^2.

This study focuses on the upper part of the Reno River basin at streamflow gauge station Casalecchio di Reno (44.47°N, 11.28°E), located just southwest of Bologna; with an extension of 1055 km^2, the basin has a rugged topography and pronounced elevation gradient, with a maximum elevation that exceeds 1750 m, and the mean elevation of 639 m (Montanari and Toth 2007).

The Reno River basin shows notable seasonal temperature changes, which reflect a temperate climate with continental influence. Summer temperatures often peak in July, and in the lowland areas they exceed 30°C. In contrast, the winter season is typically cold, with temperatures down to −8.9°C in the mountainous areas. Hydrological processes are greatly influenced by temperature fluctuations, especially in mountainous sub-basins where seasonal streamflow depends on snow and snowmelt dynamics.

The Reno River basin receives, on average, 1300 mm of precipitation annually. The Reno basin shows a strong seasonal hydrological pattern affected by Mediterranean influences as well as the Apennine climatic zone. Two peak flows in precipitation, which fall in the autumn and spring, define this pattern; the dry season occurs from June to August. Yet there is a notable variation in the total precipitation across the basin: mountainous areas receive between 1500 and 2000 mm annually, whereas the lowland area receives between 600 and 800 mm annually.

The discharge follows the same strong pattern as precipitation. Human activities – namely, dam building in the upper part of the basin – have changed the hydrological response, especially through the development of extensive lowland irrigation regions. In the Reno River basin, the Suviana hydroelectric dam is the largest reservoir, with a total capacity of 43.85×10^6 m^3 and a reservoir area of 1.49 km^2 (ARPAE 2009).

3 Data

Different precipitation datasets, presented in Table 1, were utilized to establish the hydrological model. For practical purposes, we concentrate on the period from 2001 to 2022, during which we have continuous records of observed streamflow data and all the precipitation-forcing time series available. Also, other forcing data necessary to set up the model are described in this section.

3.1 Precipitation datasets

3.1.1 ERG5 (reference data)

The ERG5 dataset is a high-resolution meteorological dataset produced by the Climate Observatory and the Territory and

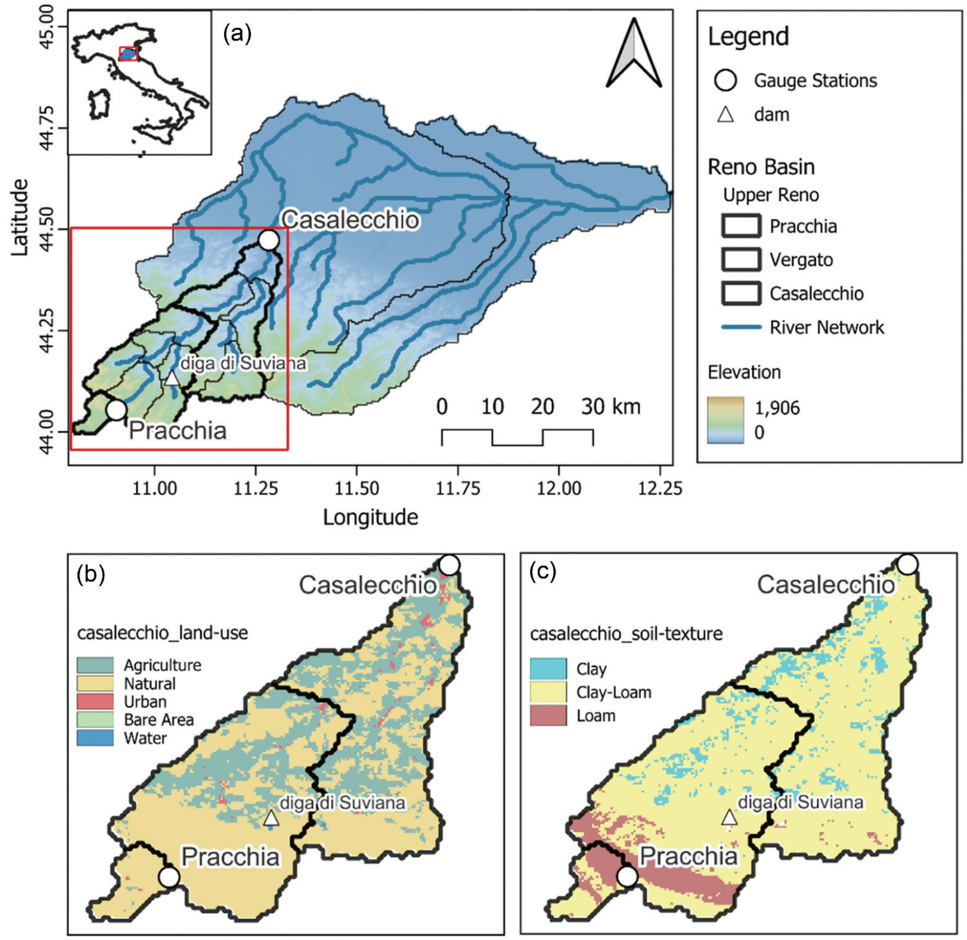

Figure 1. Study area: (a) location of the streamflow gauge stations and sub-basin used in the HYPE model (thin lines); (b) major land use classes within the Casalecchio sub-basin, from Climate Change Initiative Land Cover (CCI-LC); (c) soil type from the SoilGrids dataset.

Table 1. Description of the four gridded precipitation datasets used.

Dataset	Variable	Resolution and coverage	Data available from	Description
ERG5	Mean precipitation (P) and mean temperature (T)	5 km, Emilia-Romagna Region	2001–present	Antolini *et al.* (2016)
E-OBS	Precipitation (P)	0.1° (~10 km), Europe	1950–present	Cornes *et al.* (2018)
ERA5-Land	Precipitation (P)	0.1° (~10 km), Global	1950–present	Muñoz-Sabater *et al.* (2021)
CHIRPS	Precipitation (P)	0.05° (~5 km), 50°S – 50°N	1981–present	Funk *et al.* (2015)

Networks Unit of Arpae for the Emilia-Romagna region of Italy (https://www.arpae.it/it, last access 31 May 2025). It provides data for the main meteorological variables from 2001 to the present. The data are obtained by spatial interpolation on a regular grid from the values detected by the network of meteorological stations. The ERG5 provides hourly and daily data over a regular grid of 5 km temporal and spatial resolution, respectively. Antolini *et al.* (2016) provide a detailed description of ERG5's methodology. Daily precipitation and temperature records, both mean values, were utilized as input in the hydrological model in this study.

3.1.2 E-OBS

E-OBS (European Observations) is a high-resolution gridded observational dataset specifically for Europe, offering meteorological data from 1950 onwards (Cornes *et al.* 2018). Based on the European Climate Assessment & Dataset station network, E-OBS provides a 100-member ensemble to estimate uncertainty and is particularly valued for its fine spatial resolution (0.1° and 0.25°) over Europe. Initially developed for validating climate model simulations in the ENSEMBLES project (Hofstra *et al.* 2008), nowadays, it is widely used for climate monitoring, assessing daily extremes, and various research applications in biology, hydrology, and other fields (Hofstra *et al.* 2009).

The E-OBS dataset provides daily data on precipitation, temperature, sea level pressure, global radiation, wind speed, and relative humidity. We use only precipitation data at a spatial resolution of 0.1° (10 km, approximately).

3.1.3 ERA-5 Land

The ERA5-Land dataset is a global high-resolution reanalysis product produced by the European Centre for Medium-Range Weather Forecasts (ECMWF) as part of the Copernicus Climate Change Service (C3S). It produces detailed information on land-surface characteristics to a fine spatial resolution of 0.1° (~9 km), across land regions (Balsamo *et al.* 2015, Muñoz-Sabater *et al.* 2021), which represents an important improvement compared to ERA5 data, at 31 km (Hersbach *et al.* 2020). Spanning from 1950 to the present, ERA5-Land offers hourly data for many hydro-meteorological variables, including precipitation, air temperature, soil moisture, and surface runoff, among others. In this study, only precipitation data were utilized, which were aggregated into daily values.

Although ERA5 provides great temporal resolution and worldwide consistency, it has certain limits, especially in areas with complex terrain where it may not completely capture localized precipitation patterns, namely in mountainous areas (Tarek *et al.* 2020). It can lead to potential biases in precipitation estimates (Nogueira 2020, Gomis-Cebolla *et al.* 2023).

3.1.4 CHIRPS

Designed for climate research and drought monitoring, CHIRPS (Climate Hazards Group InfraRed Precipitation with Station data) is a high-resolution, long-term precipitation dataset (Funk *et al.* 2015). With data available from 1981 to the present at a spatial resolution of 0.05°, CHIRPS spans all longitudes from 50°S to 50°N latitude. CHIRPS provides daily and monthly data, combining satellite imagery with in situ station data. In this study, daily values were used.

Designed specifically for agricultural drought monitoring and global environmental change analysis, several studies have shown that CHIRPS most of the time underestimates the precipitation rates, in different regions (Liu *et al.* 2019, López-Bermeo *et al.* 2022, Du *et al.* 2024).

3.2 Observed discharge data

We focus on the upper part of the Reno River basin, specifically at the Casalecchio di Reno station, where long discharge records are available. Also, records are available for the Pracchia station, the headwater of the basin (Fig. 1, panel a; White dots). Both stations provide discharge records spanning from 1924 to 2022, which were gathered via the Arpae, Dext3r website (https://simc.arpae.it/dext3r/). This analysis was performed for the common period of 2001 to 2022, which coincides with the daily precipitation records starting in 2001.

3.3 Other forcing data

3.3.1 Land cover

Created by the European Space Agency (ESA), the Climate Change Initiative Land Cover (CCI-LC) dataset offers worldwide and high-resolution land cover maps for climate modelling and environmental monitoring (Harper *et al.* 2023). Covering the period from 1992 to the present, the dataset provides annual land cover classifications at 300 m spatial resolution. In this study, the map for 2020 was used.

The CCI-LC maps contain 22 classes spanning important land cover types, such as forests, croplands, grasslands, wetlands, urban areas, and water bodies. The CCI-LC product is open access and available on the website (http://maps.elie.ucl.ac.be/CCI/viewer/download.php, last access: 31 May 2025).

3.3.2 Soil texture

Developed by ISRIC – World Soil Information, the SoilGrids dataset provides world soil attributes and classes at multiple standard depths (Hengl *et al.* 2017). High-resolution (in the present study, we utilize the 250 m product) spatial estimates of important soil characteristics, including sand and clay fractions, and soil organic carbon, among others, are provided by this dataset.

Hydrological modelling depends substantially on the dataset since soil properties greatly influence infiltration rates, water retention, percolation, and runoff generation. Therefore, we employed the freely available soil grid data provided by the ISRIC data portal (web).

4 Methodology

4.1 Analysis of precipitation data

First, the precipitation data of each product are analysed. We calculate the mean precipitation at the sub-basin scale for each of the four gridded datasets, described in Section 3.1, to evaluate and compare the distribution of precipitation across the basin; also, the total precipitation for the whole basin was obtained. We did this by using the area-weighted average method, which takes into consideration the fraction of area coverage of each precipitation cell within a certain sub-basin. This method provides a better representation of precipitation patterns.

$$P_{mean,s} = \frac{\sum_{i=1}^{n} A_i \times P_i}{\sum_{i=1}^{n} A_i} \quad (1)$$

where $P_{mean,s}$ is the mean precipitation for each sub-basin, P_i is the precipitation for the grid cell i, A_i is the grid cell area within the sub-basin, and n is the total number of grid cells that lie within each sub-basin.

The E-OBS and ERA5 datasets have a coarse spatial resolution of 0.1°. No interpolation techniques were used to keep the original data accurate and prevent adding patterns or biases. This strategy ensures that the analysis shows the inherent features and uncertainties of the original datasets, not the uncertainties that come from resampling or interpolation methods. We want to give a more accurate and clearer picture of how precipitation changes and how it affects hydrological modelling by keeping its original resolution.

4.1.1 Uncertainty in precipitation datasets

To evaluate the variability and capture the seasonality across the different datasets, we calculate the absolute uncertainty following an approach similar to that presented by Biemans *et al.* (2009) and Sperna Weiland *et al.* (2015). The objective of this study is not to carry out an exhaustive analysis of the data quality of each dataset; therefore, we assume that uncertainty is represented by the differences in the precipitation values of these datasets. It is represented by the absolute range of precipitation, which is established as follows:

$$\Delta U_{abs} = P_{max,m,b} - P_{min,m,b} \quad (2)$$

$$P_{max,m,b} = \max\left(P_{mean1,b}, \ \ldots, P_{mean,4,b}\right) \quad (3)$$

where $P_{max,b}$ is the maximum mean precipitation value, from the four datasets, for the month m per the sub-basin b, and similarly $P_{min,b}$ is the minimum mean precipitation value.

In addition to the absolute uncertainty, we also calculate the relative range as a percentage, which is defined as the ratio between the absolute uncertainty range and the reference precipitation, in this case the ERG5 values. This normalization allows us to compare the variability at different time scales and sub-basins, similar to Sperna Weiland *et al.* (2015). The relative range is defined as follows:

$$\Delta U_{rel}\ [\%] = 100 \times \frac{\Delta U_{abs}}{P_{ref,b}} \tag{4}$$

where ΔU_{abs} is the absolute uncertainty range, and $P_{ref,b}$ is the mean precipitation from the ERG5 dataset for the sub-basin b. Both the absolute and relative uncertainty ranges were calculated monthly to consider the seasonality.

To complement our analysis, we also calculate the uncertainty, $U_{m,b}$, following the approach outlined by Tang *et al.* (2023, 2025).

$$U_{m,b} = \frac{\bar{\sigma}_m}{\bar{\mu}_m} \tag{5}$$

where σ is the standard deviation calculated using all datasets, and μ represents the mean value for the month m per sub-basin b. The terms σ and μ refer to mean values of the standard deviations and mean, respectively.

4.2 Hydrological modelling framework

4.2.1 Description of the HYPE model

The Hydrological Predictions for the Environment (HYPE) model, developed by the Swedish Meteorological and Hydrological Institute (SMHI), is a semi-distributed and process-based hydrological model used for the assessment of water resources and water quality at small and large scales (Lindström *et al.* 2010). The model evolved from its precursor, the Hydrologiska Byråns Vattenbalansavdelning (HBV) model (Lindström 1997).

Initially designed to evaluate water quality, HYPE has expanded its functionality to include operational drought and flood forecasting within Sweden. Recently, it has been applied at the global scale (Arheimer *et al.* 2020) and to other climatic regions (Pechlivanidis and Arheimer 2015, Andersson *et al.* 2017, Arciniega-Esparza *et al.* 2022).

The model is capable of simulating water balance and nutrient fluxes on a daily or sub-daily scale, utilizing precipitation and temperature data as primary inputs. It describes major water pathways and fluxes within a catchment or sub-catchment, ensuring the conservation of mass at each time step. Furthermore, parameters within the model are often associated with physiographic attributes, such as soil texture and land cover.

In addition to modelling natural hydrological processes, HYPE also incorporates simulations of water management practices. For instance, it can simulate regulated lakes or reservoirs with specific target release parameters. Moreover, the model includes the capability to simulate irrigation based on calculated crop water demands, which are determined by different methods integrated within the model's configuration.

For a comprehensive understanding of the HYPE model, including its methodologies and open-access code, please refer to the detailed description by Lindström *et al.* (2010) and visit https://hypeweb.smhi.se/model-water/ (last access: 31 May 2025).

4.2.2 Model set-up

To quantify the propagation of uncertainty from precipitation inputs to streamflow simulations, we use the HYPE model. While maintaining the same temperature forcing from the ERG5 dataset for all simulations, the model was forced with the gridded precipitation datasets mentioned in Section 3.1. This method isolates the impact of precipitation variability on hydrological responses.

The HYPE model works with hydrological response units (HRUs), which are the finest calculation unit in each catchment (Arheimer *et al.* 2020); each HRU is defined by the combination of land cover and soil properties. For the case of the Reno River basin, not all the land cover classes described in Section 3.3 were found. In addition, to reduce the number of model parameters, the land cover data was grouped and reclassified into the four most dominant categories (Fig. 1, panel b), where the major land use is natural cover (63%) and the second one is agriculture (33%). Urban areas and bare areas represent around 4% of the basin area. Similarly, only the three dominant soil types (Fig. 1, panel c) were considered: clay-loam type covers almost most of the basin (84%), while loam type and clay represent 6% and 10%, respectively.

The Reno River basin was divided into three main sub-basins (Fig. 1, panel a; sub-basins with thick lines); then, these sub-basins were sub-divided into 12 small sub-basins (thin lines in Fig. 1 panel a) to include the Suviana reservoir, which was simulated as a lake within the HYPE model. Twelve HRUs were obtained from the combination of land uses and soil types.

Due to a lack of a priori data regarding some information utilized in the parameterization of hydrological models, a calibration process is essential to determine the optimal parameter configurations. The Monte Carlo (MC) routine by stages in the HYPE model was utilized for this objective. For a detailed description of the algorithm application, see the documentation available on the HYPE website (http://hype.smhi.net/wiki/doku.php, last access 31 May 2025). This consists of running the model configuration, starting with a random parameter space of 100 combinations following a normal distribution; in each run the best 30 simulations (behavioural solutions) are selected and stored for the next iteration. From those a new search space is generated, and this process is repeated until 10 iterations are completed. A total of 30 000 simulations were carried out.

Each experiment was independently calibrated for each precipitation dataset. The calibration period was established as 2001 to 2010, and the validation period spans from 2011 to 2022.

4.2.3 Assessment of streamflow simulations

To evaluate the performance of the simulations, a comparison against observed streamflow was made. For it, we use the Kling-Gupta efficiency (KGE) (Gupta *et al.* 2009) criterion to quantify the similarity of the simulated and observed time series.

$$\mathrm{KGE} = 1 - \sqrt{(\mathrm{r}-1)^2 + (\alpha-1)^2 + (\beta-1)^2}, \qquad (6)$$

$$\alpha = \frac{\mu_s}{\mu_o}\ , \qquad (7)$$

$$\beta = \frac{\sigma_s}{\sigma_o}\ , \qquad (8)$$

where r is the Pearson's correlation coefficient; α is the bias component; β is the component that represents the variability; μ and σ represent the mean and standard deviation; and subscripts "s" and "o" denote the simulated and observed streamflow, respectively.

We selected the original KGE formulation over modified ones because the objective of this study is to evaluate the ability of the model to accurately represent the entire range of streamflow dynamics, including both high and low flows.

4.2.3.1 Additional hydrological signatures. In addition to the KGE, we examined additional hydrological signatures to get a deeper understanding of the model performance. We particularly investigated the mean monthly streamflow to evaluate the ability of the model to reproduce the seasonality.

We also computed the daily flow duration curves (FDC) to investigate the temporal distribution of the discharge. From the FDC, key percentiles are analysed, especially those related to the low (Q_{95}, Q_{90}, Q_{80}), the medium (Q_{50}), and the high flows (Q_{05}). These additional metrics offer critical insights that extend beyond overall model efficiency, especially in evaluating performance under diverse hydrological conditions and detecting potential biases in the simulation of extreme events (floods and droughts).

4.2.4 Uncertainty analysis for simulated streamflow

Two sets of simulations were employed to evaluate the performance and uncertainty of the hydrological model. First, the optimal simulation was identified with the highest KGE score throughout the calibration period, indicating the optimal parameter configuration. Second, an ensemble of behavioural simulations was also selected, encompassing the 30 parameter sets that satisfied a predetermined threshold within the MC routine in the HYPE model (Section 4.2.2). These behavioural simulations offer a comprehensive evaluation of the simulated streamflow uncertainty.

Like the precipitation uncertainty analysis, the absolute uncertainty in simulated streamflow was calculated (Equation 2) for the optimal simulation, and the relative uncertainty range (Equation 4) was computed using as reference the observed discharge data for Pracchia and Casalecchio stations.

5 Results

5.1 Precipitation comparison

Figure 2 shows the yearly total precipitation. The ERG5 dataset (reference) reported on average 1327.68 mm year^{-1}, and E-OBS (1292.73 mm year^{-1}) showed the closest values every year and the mean value over the analysed period. Then ERA5 (1068.49 mm year^{-1}) follows the same variability as ERG5 and E-OBS, but the values are slightly underestimated, 20% less precipitation than the ERG5 dataset.

On the other hand, CHIRPS (791.27 mm year^{-1}) always underestimates total annual precipitation, with a mean precipitation value 40% lower than the reference dataset. The variability of the adjusted values demonstrates substantial enhancement. Nonetheless, significant disparities persist, especially at the beginning of the period (from 2001 to 2007), where the values are overestimated, except in 2004. Conversely, towards the end of the period, particularly in 2019 (by around 20%), the values are significantly underestimated, similar for 2020 and 2021, although these differences are less pronounced.

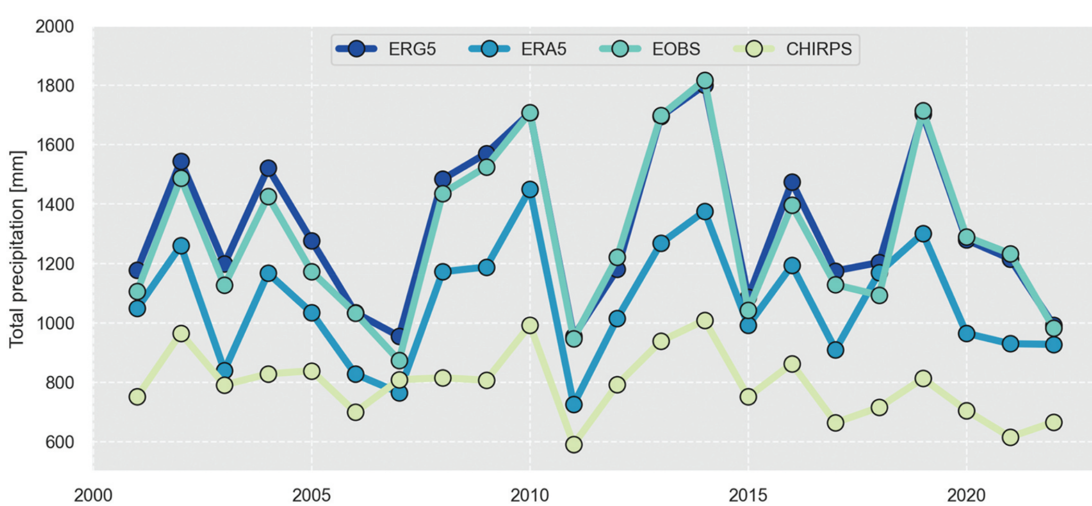

Figure 2. Total precipitation over the whole sub-basin per year for the four datasets.

After evaluating the total and mean annual precipitation, the seasonality was also compared across the different datasets (upper panel in Fig. 3). Thus, monthly mean values were computed. In Fig. 3, panel a), the solid lines represent the ERG5 values (used as reference) for each sub-basin, and the shadow areas represent the absolute range of precipitation (Equation 2). Both sub-basins follow the same dynamics: large precipitation values for the winter months and lower values are registered for summer months; however, the Pracchia sub-basin (panel b in Fig. 3) shows a large range of uncertainty, on average approximately 2 times higher compared with the whole sub-basin (Casalecchio, panel c in Fig. 3).

Similar to the annual precipitation pattern, the E-OBS dataset (green line in panels b and c, Fig. 3) shows practically the same values compared to ERG5; ERA5 reproduces the overall dynamic, but the wet season is substantially underestimated. The absolute range between datasets (difference between the lower and upper values) averages 94 mm in Pracchia and 40 mm in Casalecchio, with minimum differences occurring during the summer months. By contrast, CHIRPS consistently shows the lowest values for nearly all months in both sub-basins.

From October to March, corresponding to the wet season, ERG5 registers the maximum values for both sub-basins. On the other hand, during the dry season, particularly in the summer months (June to August), in general, all values are close to the reference dataset, especially in Pracchia. In the case of Casalecchio, ERA5 registers higher values for this period. CHIRPS considerably underestimates precipitation for all months, but especially for the wet season; for the summer months (June to August), and only for the Casalecchio sub-basin, values are close to the reference, while for Pracchia, the values are also underestimated, although to a lesser extent.

5.2 Model performance

To evaluate the model performance, the HYPE model uses the KGE as an objective function to find the optimal configuration; in this case, both the Pracchia and Casalecchio stations were used, thus the average KGE value was used as a global performance metric. Table 2 reports the average KGE obtained for the different experiments (precipitation forcing) for the calibration and validation periods. Since the Suviana reservoir area is fairly small compared to the entire basin (around 1%), the influence of the reservoir was not reflected in the downstream Casalecchio station, as suggested by the KGE values.

Overall, the model's performance is acceptable for almost all precipitation datasets, with KGE scores above 0.5, except for CHIRPS, which shows the lowest performance (KGE equal to 0.27). ERG5 (reference) and E-OBS datasets produce similar KGE scores for both periods. For all the experiments, the KGE for the validation period is slightly lower, but only ERG5 and E-OBS show values above 0.5. This demonstrates the model's ability to reproduce the hydrological response under different conditions.

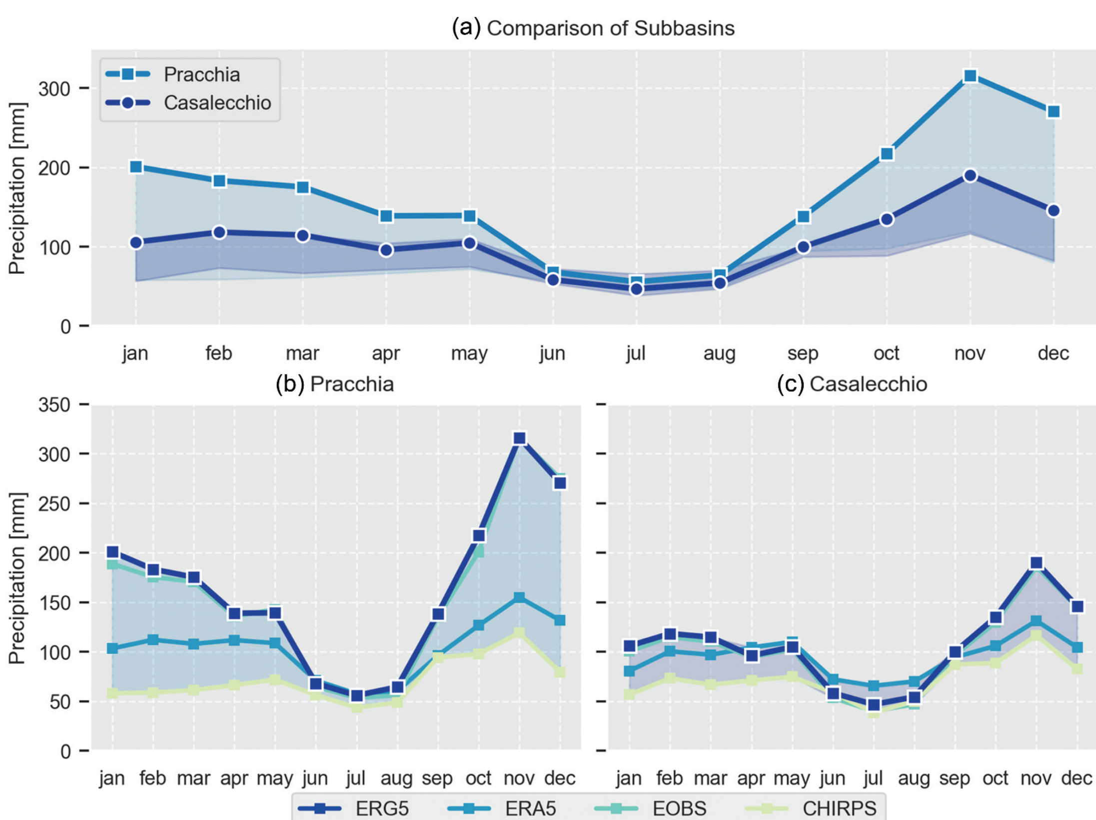

Figure 3. Range of mean monthly precipitation for the four datasets, period (2001–2022). Panel (a) Comparison of the two sub-basins: the solid lines represent the ERG5 values (reference), and shaded areas indicate the range between the different datasets for each sub-basin. Panels (b) and (c) show the mean monthly values for the different datasets for Pracchia and Casalecchio, respectively.

Table 2. Average KGE values for the calibration and validation period for each precipitation forcing.

Period/dataset	ERG5	E-OBS	ERA-5	CHIRPS
Calibration	0.79	0.78	0.52	0.27
Validation	0.75	0.75	0.48	0.27

5.2.1 Model calibration

Figure 4 shows and summarizes the resulting daily time series for each precipitation dataset, for the calibration period, 2001–2010, for both sub-basins. The upper panels (1.a and 2.a) in Fig. 4 illustrate the calibration outcomes using the ERG5 precipitation dataset. This experiment provided the highest KGE scores for both sub-basins, as displayed in each panel. For the Casalecchio sub-basin (panel 1.a), the simulated streamflow demonstrates good agreement with the observed data across both wet and dry seasons. This alignment can be observed in the optimal simulation (solid blue line), as well as across the ensemble of behavioural simulations (shaded blue area). For the headwater Pracchia (2.a), the simulated streamflow for the wet season tends to be slightly overestimated; in contrast, during the dry season, simulated values are more consistent with the observations.

The results using the E-OBS data (panels 1.b and 2.b) produced similar patterns and KGE scores to the ERG5 data; however, notable discrepancies arise at the end of the dry season, where the simulated streamflow tends to be slightly overestimated in both sub-basins. It is also noteworthy that the range of the ensemble of simulations (shaded blue area) is broader compared to the ERG5 data, particularly during the dry season.

The streamflow simulated by ERA5 data (panels 1.c and 2.c in Fig. 4) indicates acceptable KGE scores, but a pronounced disparity in streamflow dynamics is found. Generally, the timing of peak flows is correctly represented, although they are typically underestimated in both sub-basins during the wet season. Conversely, during the dry season, flows are considerably overestimated, which is also evident in the range of the ensemble simulations (shaded blue area). A similar situation arises with the streamflow simulated using CHIRPS (panels 1.d and 2.d), where the wet season tends to be roughly well represented, but the dry season shows large shifts, leading to a different inter-annual variability signal, and a less pronounced range (shaded blue area), compared to ERG5 and E-OBS. Streamflow simulated by CHIRPS forcing produced the lowest KGE values for all the precipitation forcing.

The monthly streamflow values for the optimal simulation obtained for each precipitation dataset are shown in Fig. S1 for Casalecchio and Fig. S2 for Pracchia (see Supplementary material). In general, all datasets reproduce the seasonal cycle, but notable differences emerge in the magnitude, particularly for the summer flows.

In Fig. 5, we compare the FDCs from the observed (solid Black line) and simulated streamflow for the behavioural simulations, including the optimal solution, using the different datasets for the calibration period. For Casalecchio (upper panels 1a and 1b, Fig. 5), all the percentiles generally show a great agreement between the observations and simulations. For high (<10th) and medium (25th < Q < 70th) percentiles, low variability is shown; ERA5 and CHIRPS slightly overestimate these percentiles, whereas ERG5 and E-OBS tend to underestimate them. However, a large variability appears in percentiles related to low flow conditions, above the 80th percentile (Fig. 5, panel 1.b); E-OBS reported lower values for all of these percentiles. ERG5 and ERA5 show similar values, and they show better agreement with the observed streamflow. The CHIRPS percentiles significantly underestimate the most extreme percentiles (above 90th).

A similar pattern is found in Pracchia (panels c and d in Fig. 5), but the variability between datasets is more pronounced. For the higher and medium percentiles (between the 5th and 30th), all the datasets register slightly overestimated streamflow. For all datasets, variability increases considerably from the 50th percentile onwards, compared to the entire basin at Casalecchio (panel a, Fig. 5). It is more evident for low-flow situations (panel d, Fig. 5), where, in general, all datasets tend to underestimate. For these percentiles, E-OBS (represented by greenish dots) shows the largest dispersion, 2 times broader than the rest of the dataset; across the different simulations, a similar pattern is found in ERG5 and but to a lesser extent. On the other hand, CHIRPS and ERA5 show less dispersion.

Overall, Fig. 5 highlights the sensitivity of streamflow simulation to different precipitation forcing, especially for the low flow conditions, and how uncertainty is propagated and amplified.

5.2.2 Model validation

Figure 6 shows the simulated daily streamflow for the validation period (2011–2022) for both sub-basins. The findings demonstrate that overall streamflow dynamics and seasonality identified during the calibration process are preserved in the validation period, highlighting the robustness of the calibrated model for both sub-basins. The ERG5 and E-OBS datasets consistently show great agreement with the observed streamflow in both basins, with high KGE values (0.791 and 0.819 for Casalecchio; 0.717 and 0.687 for Pracchia). ERA5 and CHIRPS simulations exhibit diminished performance, especially CHIRPS in Pracchia (KGE = 0.216), where streamflow is considerably underrepresented across time (panel 2d in Fig. 6).

For the Casalecchio sub-basin, the KGE scores obtained from the validation are similar to but slightly lower than those from the calibration period for all the datasets; only CHIRPS shows a notable difference between these periods (KGE decreases by 0.14). In contrast, for the Pracchia sub-basin, CHIRPS exhibits slightly higher KGE compared to the calibration period.

Figure 7 presents the monthly streamflow only for the optimal simulation, from each precipitation dataset and sub-basin. For both sub-basins, the seasonality is overall well represented by ERG5, E-OBS; while CHIRPS and ERA5 (yellowish and light blue boxes, respectively) considerably

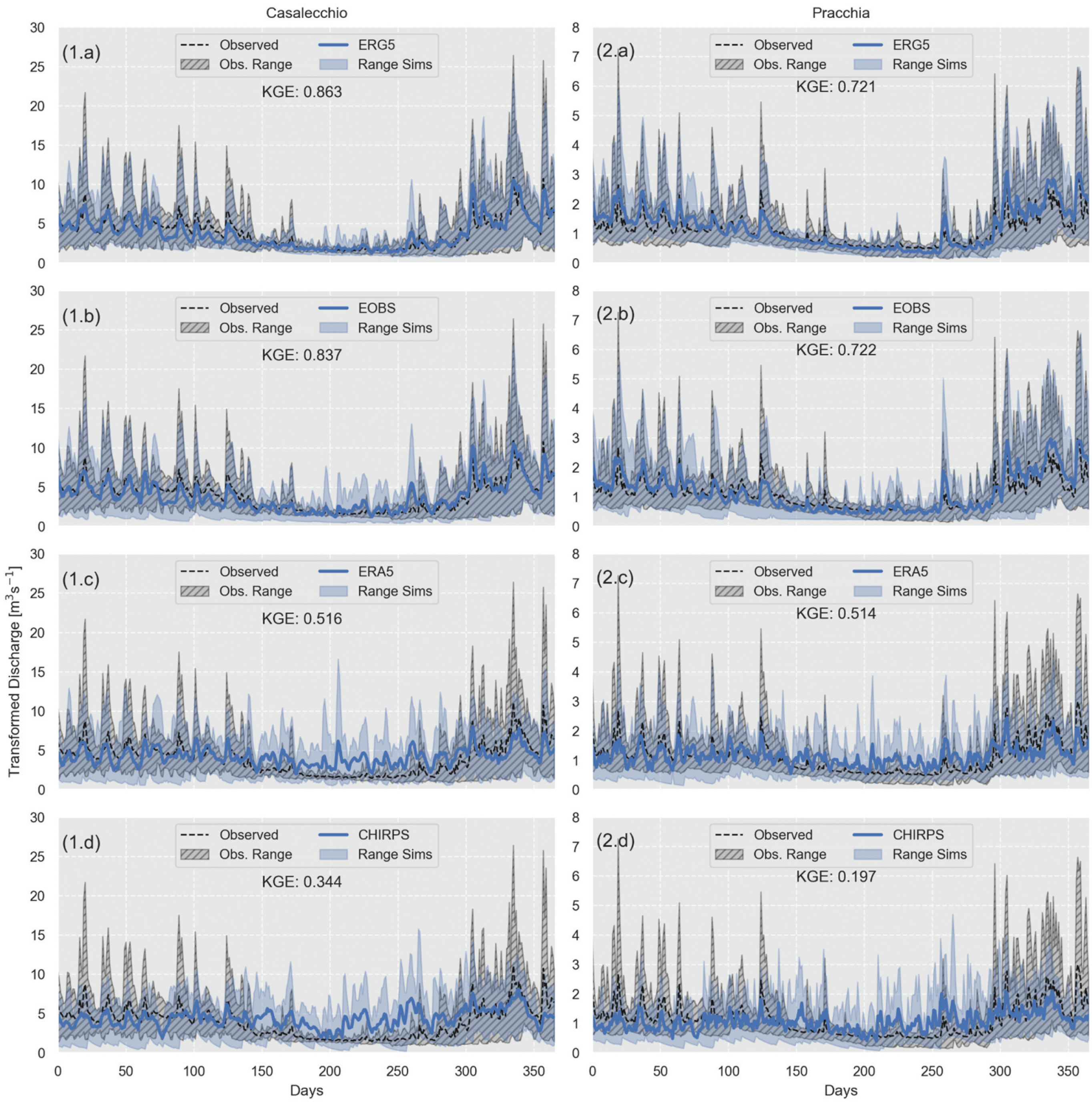

Figure 4. Simulated daily discharge for the calibration period (2001–2010) for each precipitation product (left: Casalecchio, right: Pracchia). The dashed Black line shows the mean observed discharge, and the solid blue line shows the mean simulated discharge. The shaded areas indicate ranges: in grey for observations and in blue for the 30 best simulations (Range Sims). Discharge values are transformed ($Q^{0.5}$) for visualization only. Kling-Gupta Efficiency (KGE) for the optimal simulation is reported in each case.

overestimate streamflow from June to October, especially in the Casalecchio basin.

For the Casalecchio sub-basin (upper panel in Fig. 7), simulated streamflow envelops the observed streamflow, however mean values are underestimated for all the datasets from January to April. Conversely, in November and December, the 10th–90th percentile range for simulated streamflow is overestimated, represented by the whiskers of each box, compared with the observed values (shaded grey area). For Pracchia, a similar pattern is found, but it is more pronounced for all the winter months (from November to March). In this sub-basin, mean values align closely with all the observed values. Overall, the HYPE model demonstrates its ability to reproduce the monthly streamflow regime reasonably well, independently of the precipitation dataset.

5.3 Uncertainty from precipitation to streamflow

Figure 8 shows the ranges for mean monthly precipitation and streamflow (optimal simulation) for each precipitation

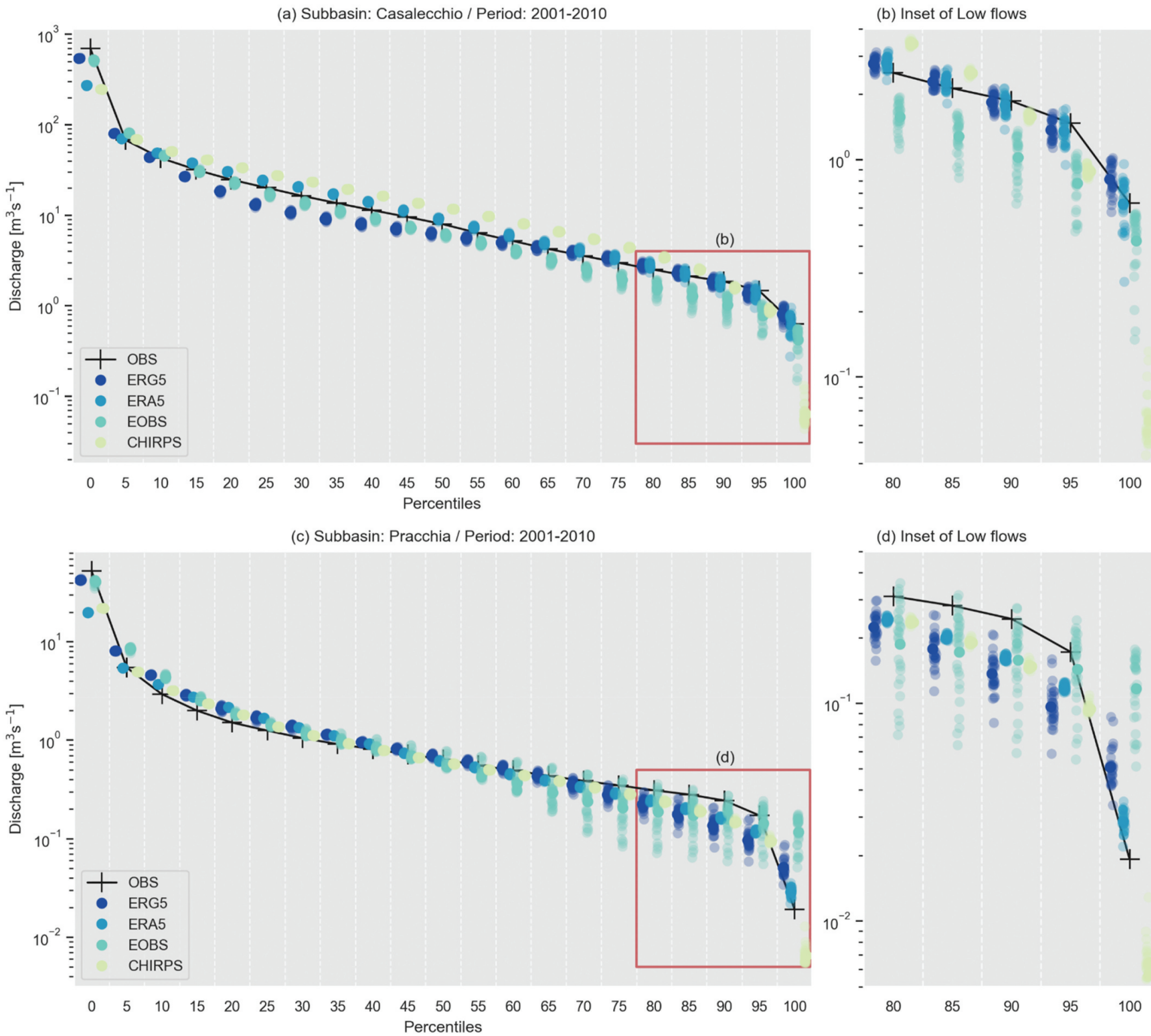

Figure 5. Flow duration curves (FDC) for all the datasets. The solid Black line shows the observed percentiles, and dots represent the 30 best simulations (from the calibration) for each dataset. Panels (a) and (b) show Casalecchio (all percentiles, and 80th – 100th only, respectively). Panels (c) and (d) show Pracchia. Note the different y-axis scale.

dataset. Regarding the uncertainty in precipitation (shaded blue areas in both panels), we found a noticeable pattern. The minimum values of the absolute uncertainty range (Equation 2) are presented from June to September for both basins: for Pracchia, 14 mm in July; and for Casalecchio, 13 mm in September. The maximum value of the absolute range occurs in November in both cases, 197 mm in Pracchia and 74 mm in Casalecchio. In terms of absolute uncertainty, Pracchia, the headwaters of the basin, has values approximately twice as high as those in Casalecchio.

When uncertainty is expressed in relative terms (Equation 4), the seasonal pattern in Pracchia remains consistent, with high values (about 70%) during the winter months (DJF), and minima (<25%) for the summer months (JJA). For Casalecchio, however, the pattern is less clear: for almost all months, relative uncertainty remains close to 40% and the minimum value is only reported for September. Although magnitudes are slightly reduced, the relative uncertainty in Pracchia is generally about 30% higher than in Casalecchio.

The uncertainty in streamflow exhibits a more complex pattern (Fig. 8). As described in Section 5.2, the streamflow dynamics are generally well represented for both basins. Consistent overestimation of streamflow is reported from August to October, regardless of the parameterization of HYPE for both sub-basins, which also translates into a slightly wider range of uncertainty compared to the other months. Although for the Casalecchio sub-basin (shaded grey area in left panel), the uncertainty

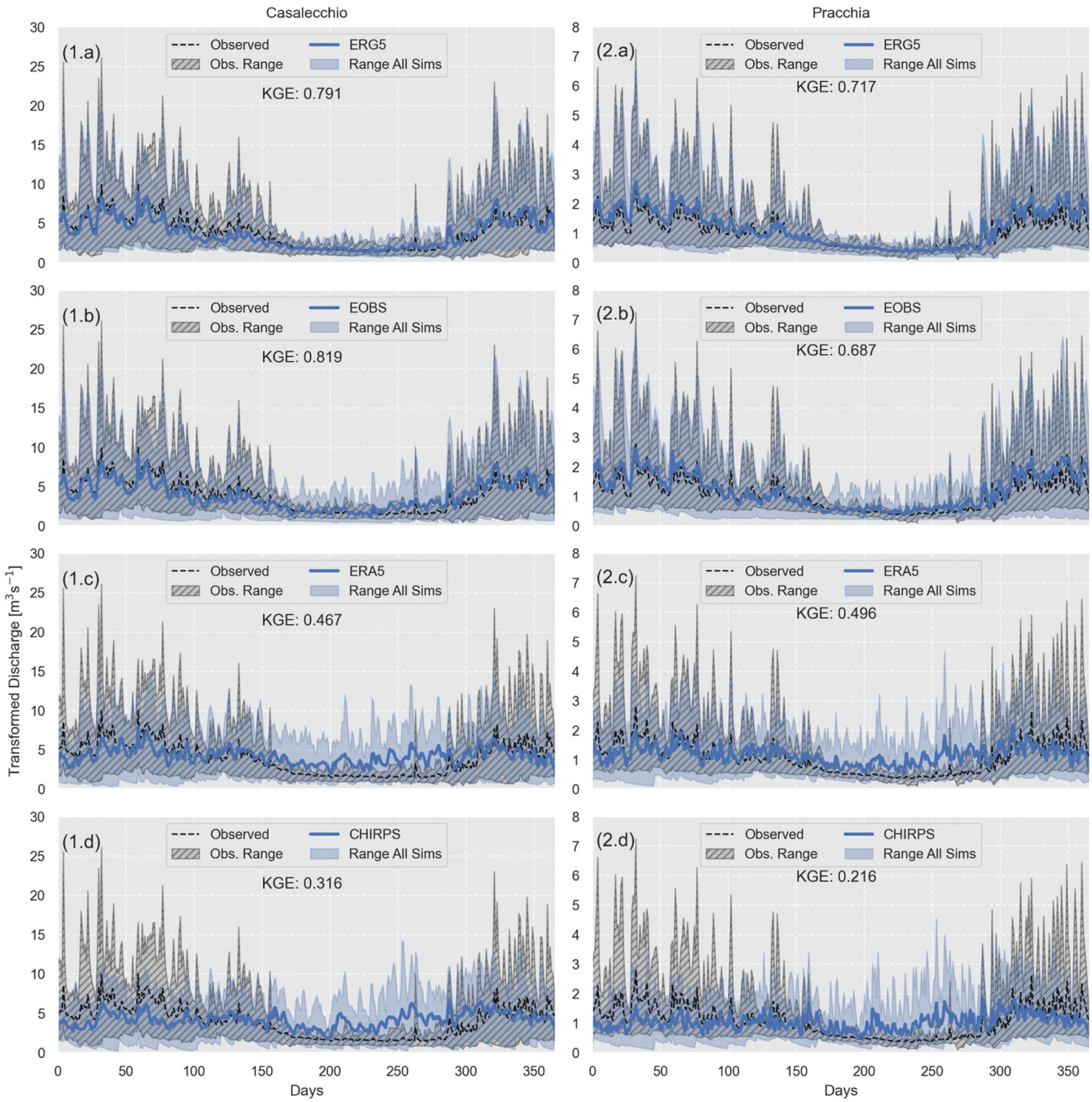

Figure 6. Simulated daily discharge for the validation period (2011–2022) for each precipitation product (left: Casalecchio, right: Pracchia). The dashed black line shows the mean observed discharge, and the solid blue line shows the mean simulated discharge. The shaded areas indicate ranges: in grey for observations and in blue for the 30 best simulations (Range Sims). Discharge values are transformed (Q0.5) for visualization only. Kling-Gupta Efficiency (KGE) for the optimal simulation is reported in each case.

range falls below the observed streamflow from January to March.

For both sub-basins, the absolute uncertainty range is comparable (values between 22 to 62 mm) for most of the months, except for the winter months (Dec to Jan) and March in Pracchia (right panel in Fig. 8), where the absolute range reported values above 90 mm, highlighting the impact of uncertainty from precipitation to streamflow in the mountainous sub-basin.

In relative terms (with Equation 4 using observed streamflow as a reference), Casalecchio reported high fluctuations across the streamflow regime, and large values (>170%) from June to October, while the rest of the months report values around 40%. For Pracchia a similar pattern is found, with higher values (>100%) from June to September, but for the rest of the months the relative uncertainty is higher (~75%).

We also quantify the ratio between streamflow and precipitation, which explains the fraction of uncertainty that translates from precipitation to streamflow. In both sub-basins, for almost all months relative uncertainty in streamflow is larger than that in precipitation (values > 1), which indicates that uncertainty is amplified. On average, relative

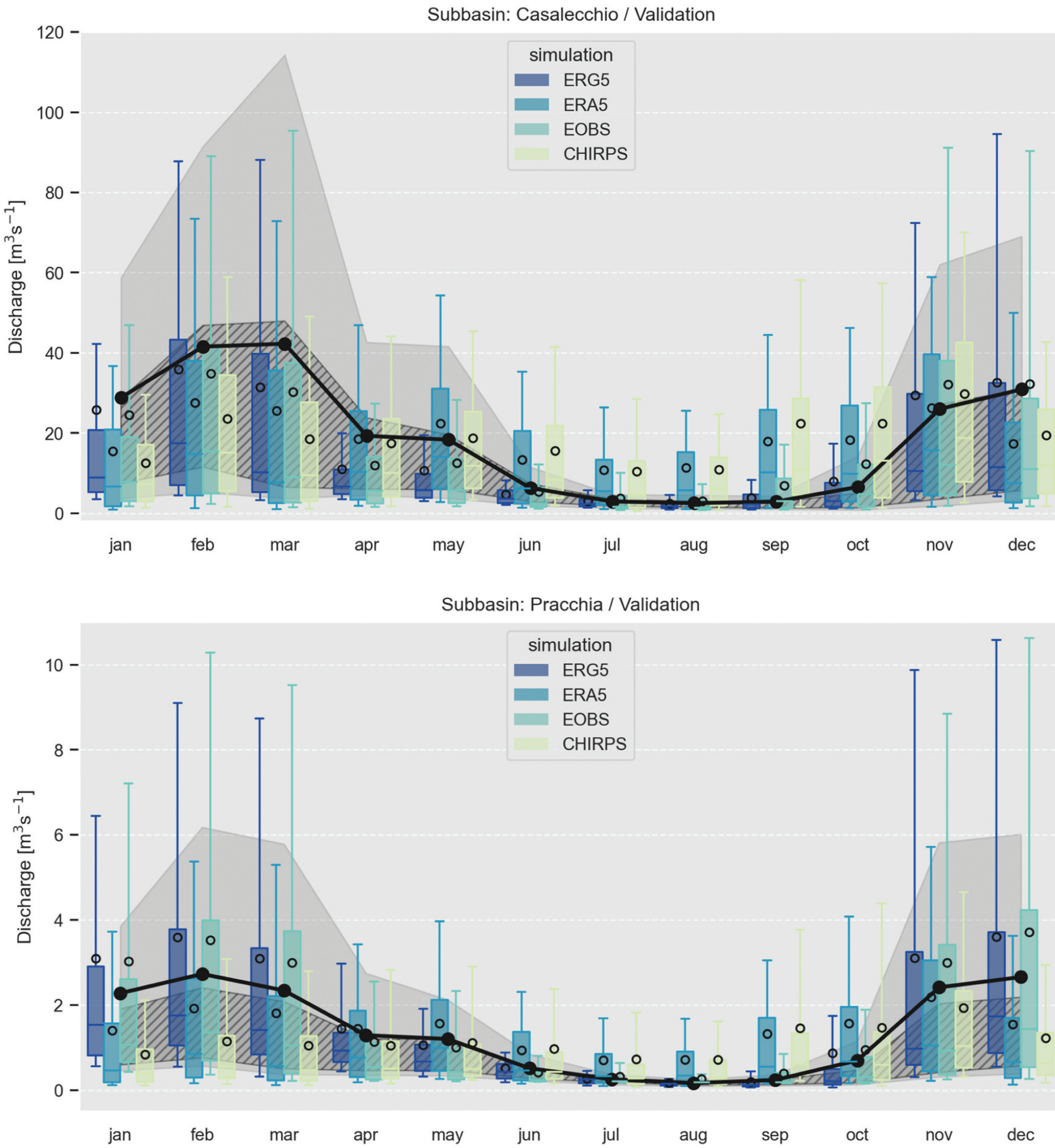

Figure 7. Monthly discharge for the optimal simulation: each box plot represents the monthly discharge simulated by each precipitation dataset. The box represents the interquartile range, and the whiskers extend from the 10th to the 90th percentile. The horizontal line in each box denotes the median, and unfilled black dots indicate the mean. The observed mean monthly values are indicated by a solid black line. The shaded light grey area indicates the 10th–90th percentile range, while the dark grey area indicates the 25th–75th percentile range.

uncertainty is amplified 2.8 times from precipitation to streamflow.

Evaluating the uncertainty using the standard deviation, $U_{m,b}$ (Equation 5), the overall pattern previously observed remains (panel a, Fig. 3). The lowest uncertainty values for precipitation in Pracchia (~0.26) occur during the dry season, and the highest values (>0.45) are registered in winter. Conversely, Casalecchio demonstrates a contrasting pattern, with maximum uncertainty in July (0.34) and reduced values averaging 0.19 across the other months.

For streamflow, in Pracchia the pattern is the opposite, exhibiting the greatest uncertainty in August and September (>0.58). For Casalecchio, during the dry season values exceed 0.55, while they average around 0.30 in the remaining months.

In both sub-basins, precipitation uncertainty is consistently amplified when propagated to streamflow, on average increased by 1.7 times. This amplification is most noticeable during the dry season, when uncertainty is roughly doubled.

6 Discussion

6.1 Uncertainty in precipitation and streamflow

Over the past few decades, there has been a proliferation of gridded precipitation datasets. These products are widely used

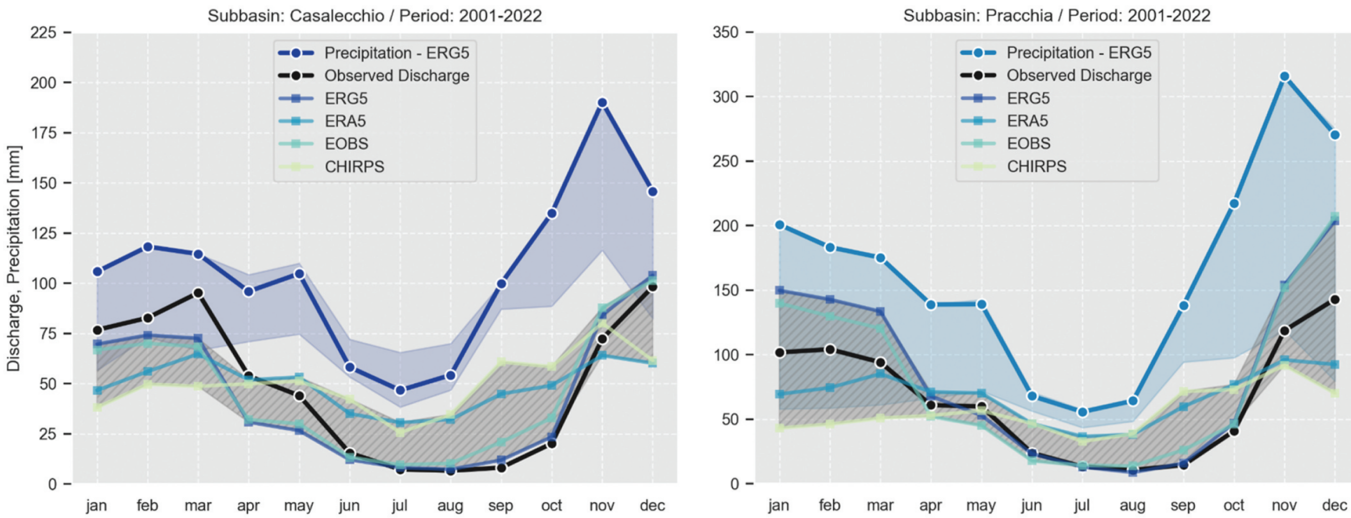

Figure 8. Mean monthly precipitation (blue shaded area: uncertainty range) and streamflow (grey shaded area: uncertainty range) for Casalecchio (left panel) and Pracchia (right panel) stations, covering the entire observation period. Note that the y-axis scales differ between the two panels.

despite inconsistencies arising from factors such as interpolation techniques, which tend to smooth out extreme values. This can affect precipitation intensities and obscure heterogeneities and trends associated with topography and atmospheric conditions (Boers *et al.* 2016).

ERG5 and E-OBS, both observational datasets, exhibit similar spatial and temporal precipitation patterns across the study area. Similar results were reported by Sarigil *et al.* (2024), but in our study the winter months (November and December) show particularly high values for the headwater, Pracchia. This could be explained by the snowfall and by heterogeneous precipitation patterns that are not fully captured by the gridded datasets (e.g. Durand *et al.* 1993, Prein and Gobiet 2017), and differences can be attributed to the interpolation algorithm used in each dataset (Merino *et al.* 2021).

On the other hand, ERA5 and CHIRPS show significant discrepancies in estimating precipitation, particularly during winter. This aligns with previous studies (e.g. Sun *et al.* 2018, Gomis-Cebolla *et al.* 2023, Sarigil *et al.* 2024). These biases directly affect the simulated streamflow, although hydrological models try to compensate for these errors during the calibration stage (e.g. Beck *et al.* 2017a, Raimonet *et al.* 2017), underscoring the need for enhanced representation of precipitation fields. Recent research has focused on improving precipitation datasets at finer spatial resolutions to enhance their applicability in hydrological modelling for water management (Cenobio-Cruz *et al.* 2024) and their impact on hydrodynamic modelling (Ochoa-Rodriguez *et al.* 2015).

In terms of streamflow, E-OBS overall demonstrates similar performance to the ERG5 dataset, but differences arise for the low flow situation, even when the precipitation patterns are very similar. This is often linked to equifinality in hydrological modelling (e.g. Beven 2012) A more thorough investigation is needed to understand how model parameterization influences its ability to compensate for deviations in precipitation inputs. Parameters governing land-surface processes are particularly important, as their effects propagate through the hydrological system more slowly than direct precipitation–runoff responses. For example, soil flow parameters may offset deficiencies in CHIRPS or ERA5 precipitation, leading to higher simulated summer flows despite underestimated rainfall. Similarly, parameters controlling snow accumulation and melt can partly explain simulated winter flows comparable to observations, even when precipitation inputs differ. Sarigil *et al.* (2024) found similar patterns in their study.

However, disentangling the contribution of parameter uncertainty and forcing uncertainty requires particular sensitivity analysis or multi-objective calibration frameworks (Fowler *et al.* 2018). A detailed assessment of these interaction is beyond the scope of this study but represents an important avenue for future research.

The uncertainty analyses using the relative range and the standard deviation show similarities. Our results show patterns consistent with previous studies, including Biemans *et al.* (2009) and Sperna Weiland *et al.* (2015), which underscores the impact of uncertainty in precipitation on simulated streamflow. Some variations are found, which might be attributed to the size of the catchment analysed here, the different precipitation datasets utilized, the hydrological model itself, and the calibration techniques employed.

Although direct comparison with Tang *et al.* (2025) is limited due to methodological and scale differences, some similarities are observed; for example, streamflow uncertainty in the downstream sub-basin is smaller compared to the upstream, which can be attributed to the routing effect. It also aligns with other studies (e.g. Pokorny *et al.* 2020, Tang *et al.* 2023).

6.2 *Limitations and future studies*

It is important to highlight that the approach presented here, while allowing us to isolate the effects of precipitation uncertainty, does not account for potential interactions between precipitation and temperature. These can play a significant role in snow-dominated sub-basins where temperature drives the dynamics of snowmelt-driven runoff (e.g. Knoben *et al.* 2020, Tang *et al.* 2023, 2025). Recent studies show that interactions in meteorological forcing are complex. Schreiner-

McGraw and Ajami (2022), for example, found that uncertainty between these forcings is cumulative. Conversely, other studies demonstrated that uncertainty associated with air temperature exerts a smaller impact than precipitation uncertainty (Dembélé *et al.* 2020, Tang *et al.* 2023). Future research is needed to unravel this complex interplay.

Although hydrological model outputs reported in this study are overall acceptable, notable differences emerged in reproducing low-flow conditions, which are predominantly controlled by hydrological soil processes (Beck *et al.* 2017b). Recent studies highlight that uncertainty arising from model structures/parameterizations is notably pronounced in the simulation of low-flow events (van Kempen *et al.* 2021, Guo *et al.* 2024). Thus, it is essential to undertake more comprehensive research into the interplay between forcing uncertainty and parameter uncertainty. Our finding suggest hydrological outputs should be used conservatively, especially for extreme events, such as drought analysis.

Moreover, the application of probabilistic methods (ensemble-based products), which provide a more comprehensive representation of variability and extremes (e.g. Cornes *et al.* 2018, Falck *et al.* 2021, Tang *et al.* 2022) should be applied in parallel for a more comprehensive forcing uncertainty quantification. In addition, future research should also incorporate more sophisticated methods, such as advanced statistical approaches or machine learning techniques (e.g. reducing computational demand in modelling or identifying complex patterns that traditional methods may overlook) to produce more robust quantification and characterization of uncertainty.

7 Conclusions

Gridded precipitation datasets have emerged and multiplied in recent decades as key tools in climate and hydrological studies. This study aims to unravel how uncertainty in these precipitation products cascades through a process-based hydrological model and influences streamflow predictions.

First, the various precipitation datasets were examined to assess temporal variations. For each dataset, we calculated total annual and seasonal precipitation at the sub-basin level throughout the 2001–2022 period, with specific attention to seasonal patterns and variability in mountainous and lowland locations. Then, the effect of input precipitation uncertainty on hydrological outputs was evaluated through simulated streamflow. With an emphasis on seasonal dynamics and variances between sub-basins, uncertainty was quantified using the range and variability of simulated streamflow. The main findings are summarized below:

(1) The precipitation variability across all the datasets is pronounced, particularly in the small and mountainous sub-basin, where uncertainty is 1.8 times higher than compared to the whole sub-basin, and this effect is also propagated and amplified to the streamflow.
(2) The results indicate that the hydrological model tends to compensate for errors in the input precipitation data, often resulting in similar streamflow responses across different datasets, particularly during the winter season. This suggests that parameter optimization can mask some of the variability in the forcing data.

The differences in precipitation, on the other hand, clearly affect the simulated streamflow. The most noticeable effects arise during the dry season, when the hydrological system is more sensitive to changes in input. The results of the study suggest:

(3) The E-OBS dataset performed comparably to the ERG5 dataset (in terms of both precipitation and simulated streamflow), confirming the reliability of ground-based products across the study area. However, consistent underperformance was reported by ERA5 and E-OBS, indicating their hydrological application is limited in this region.
(4) Uncertainty in streamflow is around 3.5 times larger than the uncertainty in precipitation inputs for the dry season. The opposite occurs for the wet season, where uncertainty decreases slightly. However, this clearly shows how hydrological processes represented by the model can amplify each other.

These findings underscore the significant effect of precipitation quality in hydrological modelling and the necessity of assessing and quantifying input uncertainty, especially in regions with complex terrain and seasonal hydrological contrasts.

Disclosure statement

No potential conflict of interest was reported by the author(s).

Funding

This research has received funding from the Horizon Europe's TRANSCEND (Transformational and Robust Adaptation to Water Scarcity and Climate Change Under Deep Uncertainty) Project, under grant agreement No. 101084110.

ORCID

Omar Cenobio-Cruz http://orcid.org/0000-0001-5841-2858
Giuliano Di Baldassarre http://orcid.org/0000-0002-8180-4996

References

Abbas, A., *et al.*, 2025. Comprehensive global assessment of 23 gridded precipitation datasets across 16,295 catchments using hydrological modeling. *EGUsphere*. doi:10.5194/egusphere-2024-4194
Alfieri, L., *et al.*, 2022. High-resolution satellite products improve hydrological modeling in northern Italy. *Hydrology and Earth System Sciences*, 26 (14), 3921–3939. doi:10.5194/hess-26-3921-2022
Andersson, J.C.M., *et al.*, 2017. Providing peak river flow statistics and forecasting in the Niger River basin. *Physics and Chemistry of the Earth, Parts A/B/C*, 100, 3–12. doi:10.1016/j.pce.2017.02.010
Andréassian, V., *et al.*, 2001. Impact of imperfect rainfall knowledge on the efficiency and the parameters of watershed models. *Journal of Hydrology*, 250 (1–4), 206–223. doi:10.1016/S0022-1694(01)00437-1
Antolini, G., *et al.*, 2016. A daily high-resolution gridded climatic data set for Emilia-Romagna, Italy, during 1961-2010. *International Journal of Climatology*, 36 (4), 1970–1986. doi:10.1002/joc.4473

Arciniega-Esparza, S., *et al.*, 2022. Remote sensing-aided rainfall–runoff modeling in the tropics of Costa Rica. *Hydrology and Earth System Sciences*, 26 (4), 975–999. doi:10.5194/hess-26-975-2022

Arheimer, B., *et al.*, 2020. Global catchment modelling using World-Wide HYPE (WWH), open data, and stepwise parameter estimation. *Hydrology and Earth System Sciences*, 24 (2), 535–559. doi:10.5194/hess-24-535-2020

ARPAE, (2009). Gli invasi di Suviana e Brasimone: Report di monitoraggio 2009 [Technical report]. Agenzia Regionale per la Protezione Ambientale dell'Emilia-Romagna. https://www.arpae.it/it/il-territorio/bologna/report-a-bo/acqua/acque-superficiali/monitoraggio-brasimone/gli-invasi-di-suviana-e-brasimone-report-monitoraggio-2009 [Accessed 31 May 2025].

Balsamo, G., *et al.*, 2015. Era-interim/land: a global land surface reanalysis data set. *Hydrology and Earth System Sciences*, 19 (1), 389–407. doi:10.5194/HESS-19-389-2015

Bárdossy, A., *et al.*, 2022. Is precipitation responsible for the most hydrological model uncertainty? *Frontiers in Water*, 4. doi:10.3389/frwa.2022.836554

Bates, B.C., *et al.*, 2008. Climate change and water. Technical paper of the Intergovernmental Panel on Climate Change, IPCC Secretariat, 210.

Beck, H.E., *et al.*, 2017a. Global evaluation of runoff from 10 state-of-the-art hydrological models. *Hydrology and Earth System Sciences*, 21 (6), 2881–2903. doi:10.5194/hess-21-2881-2017

Beck, H.E., *et al.*, 2017b. Global-scale evaluation of 22 precipitation datasets using gauge observations and hydrological modeling. *Hydrology and Earth System Sciences*, 21 (12), 6201–6217. doi:10.5194/HESS-21-6201-2017

Beven, K., 2012. Parameter estimation and predictive uncertainty. In: *Rainfall-runoff modelling*. Wiley, 231–287. doi:10.1002/9781119951001.ch7.

Beven, K. and Binley, A., 1992. The future of distributed models: model calibration and uncertainty prediction. *Hydrological Processes*, 6 (3), 279–298. doi:10.1002/hyp.3360060305

Biemans, H., *et al.*, 2009. Effects of precipitation uncertainty on discharge calculations for main river basins. *Journal of Hydrometeorology*, 10 (4), 1011–1025. doi:10.1175/2008JHM1067.1

Boers, N., *et al.*, 2016. Spatiotemporal characteristics and synchronization of extreme rainfall in South America with focus on the Andes Mountain range. *Climate Dynamics*, 46 (1–2), 601–617. doi:10.1007/s00382-015-2601-6

Camici, S., *et al.*, 2018. How reliable are satellite precipitation estimates for driving hydrological models: a verification study over the Mediterranean area. *Journal of Hydrology*, 563, 950–961. doi:10.1016/j.jhydrol.2018.06.067

Cammalleri, C., *et al.*, 2024. Testing trends in gridded rainfall datasets at relevant hydrological scales: a comparative study with regional ground observations in southern Italy. *Journal of Hydrology: Regional Studies*, 55, 101950. doi:10.1016/j.ejrh.2024.101950

Cavalleri, F., *et al.*, 2024. Multi-scale assessment of high-resolution reanalysis precipitation fields over Italy. *Atmospheric Research*, 312, 107734. doi:10.1016/j.atmosres.2024.107734

Cenobio-Cruz, O., *et al.*, 2024. Assessment of the hydrological impact of an hourly precipitation distribution correction method in the SASER modeling system. *Journal of Hydrology*, 635, 131136. doi:10.1016/j.jhydrol.2024.131136

Clark, M.P., *et al.*, 2015. A unified approach for process-based hydrologic modeling: 1. Modeling concept. *Modeling Concept. Water Resources Research*, 51 (4), 2498–2514. doi:10.1002/2015WR017198

Clark, M.P., *et al.*, 2016. Characterizing uncertainty of the hydrologic impacts of climate change. *Current Climate Change Reports*, 2 (2), 55–64. doi:10.1007/s40641-016-0034-x

Clark, M.P., *et al.*, 2017. The evolution of process-based hydrologic models: historical challenges and the collective quest for physical realism. *Hydrology and Earth System Sciences*, 21 (7), 3427–3440. doi:10.5194/hess-21-3427-2017

Cornes, R.C., *et al.*, 2018. An ensemble version of the E-OBS temperature and precipitation data sets. *Journal of Geophysical Research: Atmospheres*, 123 (17), 9391–9409. doi:10.1029/2017JD028200

Dembélé, M., *et al.*, 2020. Suitability of 17 gridded rainfall and temperature datasets for large-scale hydrological modelling in West Africa. *Hydrology and Earth System Sciences*, 24 (11), 5379–5406. doi:10.5194/hess-24-5379-2020

Di Baldassarre, G. and Montanari, A., 2009. Uncertainty in river discharge observations: a quantitative analysis. *Hydrology and Earth System Sciences*, 13 (6), 913–921. doi:10.5194/HESS-13-913-2009

Döll, P., *et al.*, 2016. Modelling freshwater resources at the global scale: challenges and prospects. *Surveys in Geophysics*, 37 (2), 195–221. doi:10.1007/s10712-015-9343-1

Du, H., *et al.*, 2024. Evaluating the effectiveness of CHIRPS data for hydroclimatic studies. *Theoretical and Applied Climatology*, 155 (3), 1519–1539. doi:10.1007/s00704-023-04721-9

Durand, Y., *et al.*, 1993. A meteorological estimation of relevant parameters for snow models. *Annals of Glaciology*, 18, 65–71. doi:10.3189/s0260305500011277

Engeland, K., *et al.*, 2016. Effects of uncertainties in hydrological modelling. A case study of a mountainous catchment in southern Norway. *Journal of Hydrology*, 536, 147–160. doi:10.1016/j.jhydrol.2016.02.036

Falck, A.S., *et al.*, 2021. Applying a precipitation error model to numerical weather predictions for probabilistic flood forecasts. *Journal of Hydrology*, 598, 126374. doi:10.1016/j.jhydrol.2021.126374

Fekete, B.M., *et al.*, 2004. Uncertainties in precipitation and their impacts on runoff estimates. *Journal of Climate*, 17 (2), 294–304. doi:10.1175/1520-0442(2004)017<0294:UIPATI>2.0.CO;2

Fowler, K., *et al.*, 2018. Simulating runoff under changing climatic conditions: A framework for model improvement. *Water Resources Research*, 54 (12), 9812–9832. doi:10.1029/2018WR023989

Funk, C., *et al.*, 2015. The climate hazards infrared precipitation with stations—a new environmental record for monitoring extremes. *Scientific Data*, 2 (1), 1–21. doi:10.1038/sdata.2015.66

Gentilucci, M., Barbieri, M., and Pambianchi, G., 2022. Reliability of the IMERG product through reference rain gauges in Central Italy. *Atmospheric Research*, 278, 106340. doi:10.1016/j.atmosres.2022.106340

Gharari, S., *et al.*, 2021. Understanding the information content in the hierarchy of model development decisions: learning from data. *Water Resources Research*, 57 (6), e2020WR027948. doi:10.1029/2020WR027948

Gomis-Cebolla, J., *et al.*, 2023. Evaluation of ERA5 and ERA5-land reanalysis precipitation datasets over Spain (1951–2020). *Atmospheric Research*, 284, 106606. doi:10.1016/J.ATMOSRES.2023.106606

Guo, H., *et al.*, 2024. Global evaluation of simulated high and low flows from 23 macroscale models. *Journal of Hydrometeorology*, 25 (3), 425–443. doi:10.1175/JHM-D-23-0176.1

Gupta, H.V., *et al.*, 2009. Decomposition of the mean squared error and NSE performance criteria: implications for improving hydrological modelling. *Journal of Hydrology*, 377 (1–2), 80–91. doi:10.1016/j.jhydrol.2009.08.003

Gupta, V.K. and Sorooshian, S., 1985. The relationship between data and the precision of parameter estimates of hydrologic models. *Journal of Hydrology*, 81 (1–2), 57–77. doi:10.1016/0022-1694(85)90167-2

Harper, K.L., *et al.*, 2023. A 29-year time series of annual 300 m resolution plant-functional-type maps for climate models. *Earth System Science Data*, 15 (3), 1465–1499. doi:10.5194/ESSD-15-1465-2023

Hengl, T., *et al.*, 2017. SoilGrids250m: global gridded soil information based on machine learning. *PLOS ONE*, 12 (2), e0169748. doi:10.1371/journal.pone.0169748

Herrera, P.A., Marazuela, M.A., and Hofmann, T., 2022. Parameter estimation and uncertainty analysis in hydrological modeling. *WIRs Water*, 9 (1), e1569. doi:10.1002/wat2.1569

Hersbach, H., *et al.*, 2020. The ERA5 global reanalysis. *Quarterly Journal of the Royal Meteorological Society*, 146 (730), 1999–2049. doi:10.1002/qj.3803

Hofstra, N., *et al.*, 2008. Comparison of six methods for the interpolation of daily, European climate data. *Journal of Geophysical Research: Atmospheres*, 113 (D21), 21110. doi:10.1029/2008JD010100

Hofstra, N., *et al.*, 2009. Testing E-OBS European high-resolution gridded data set of daily precipitation and surface temperature. *Journal of*

Geophysical Research: Atmospheres, 114 (D21), 21101. doi:10.1029/2009JD011799

Kabir, T., Pokhrel, Y., and Felfelani, F., 2022. On the precipitation-induced uncertainties in process-based hydrological modeling in the Mekong River Basin. *Water Resources Research*, 58 (2), e2021WR030828. doi:10.1029/2021WR030828

Kidd, C. and Huffman, G., 2011. Global precipitation measurement. *Meteorological Applications*, 18 (3), 334–353. doi:10.1002/met.284

Knoben, W.J.M., *et al.*, 2020. A brief analysis of conceptual model structure uncertainty using 36 models and 559 catchments. *Water Resources Research*, 56 (9), e2019WR025975. doi:10.1029/2019WR025975

Lindström, G., 1997. A simple automatic calibration routine for the HBV model. *Hydrology Research*, 28 (3), 153–168. doi:10.2166/nh.1997.0009

Lindström, G., *et al.*, 2010. Development and testing of the HYPE (Hydrological Predictions for the Environment) water quality model for different spatial scales. *Hydrology Research*, 41 (3–4), 295–319. doi:10.2166/nh.2010.007

Liu, J., *et al.*, 2019. Evaluation and comparison of CHIRPS and MSWEP daily-precipitation products in the Qinghai-Tibet Plateau during the period of 1981–2015. *Atmospheric Research*, 230, 104634. doi:10.1016/J.ATMOSRES.2019.104634

Longo-Minnolo, G., *et al.*, 2022. Assessing the use of ERA5-land reanalysis and spatial interpolation methods for retrieving precipitation estimates at basin scale. *Atmospheric Research*, 271, 106131. doi:10.1016/j.atmosres.2022.106131

López-Bermeo, C., *et al.*, 2022. Validation of the accuracy of the CHIRPS precipitation dataset at representing climate variability in a tropical mountainous region of South America. *Physics and Chemistry of the Earth, Parts A/B/C*, 127, 103184. doi:10.1016/J.PCE.2022.103184

Mankin, K.R., *et al.*, 2025. Review of gridded climate products and their use in hydrological analyses reveals overlaps, gaps, and the need for a more objective approach to selecting model forcing datasets. *Hydrology and Earth System Sciences*, 29 (1), 85–108. doi:10.5194/hess-29-85-2025

McMillan, H., Krueger, T., and Freer, J., 2012. Benchmarking observational uncertainties for hydrology: Rainfall, river discharge and water quality. *Hydrological Processes*, 26 (26), 4078–4111. doi:10.1002/hyp.9384

McMillan, H.K., Westerberg, I.K., and Krueger, T., 2018. Hydrological data uncertainty and its implications. *WIRs Water*, 5 (6), e1319. doi:10.1002/wat2.1319

Merino, A., *et al.*, 2021. Evaluation of gridded rain-gauge-based precipitation datasets: impact of station density, spatial resolution, altitude gradient and climate. *International Journal of Climatology*, 41 (5), 3027–3043. doi:10.1002/JOC.7003

Moges, E., *et al.*, 2021. Review: Sources of hydrological model uncertainties and advances in their analysis. *Water*, 13 (1), 28. doi:10.3390/w13010028

Montanari, A. and Di Baldassarre, G., 2013. Data errors and hydrological modelling: The role of model structure to propagate observation uncertainty. *Advances in Water Resources*, 51, 498–504. doi:10.1016/J.ADVWATRES.2012.09.007

Montanari, A. and Toth, E., 2007. Calibration of hydrological models in the spectral domain: an opportunity for scarcely gauged basins? *Water Resources Research*, 43 (5), 1–10. doi:10.1029/2006WR005184

Muñoz-Sabater, J., *et al.*, 2021. Era5-land: a state-of-the-art global reanalysis dataset for land applications. *Earth System Science Data*, 13 (9), 4349–4383. doi:10.5194/ESSD-13-4349-2021

Nikolopoulos, E.I., *et al.*, 2010. Understanding the scale relationships of uncertainty propagation of satellite rainfall through a distributed hydrologic model. *Journal of Hydrometeorology*, 11 (2), 520–532. doi:10.1175/2009JHM1169.1

Nogueira, M., 2020. Inter-comparison of ERA-5, ERA-Interim and GPCP rainfall over the last 40 years: process-based analysis of systematic and random differences. *Journal of Hydrology*, 583, 124632. doi:10.1016/J.JHYDROL.2020.124632

Ochoa-Rodriguez, S., *et al.*, 2015. Impact of spatial and temporal resolution of rainfall inputs on urban hydrodynamic modelling outputs: a multi-catchment investigation. *Journal of Hydrology*, 531, 389–407. doi:10.1016/j.jhydrol.2015.05.035

Pappenberger, F., Thielen, J., and Del Medico, M., 2011. The impact of weather forecast improvements on large scale hydrology: analysing a decade of forecasts of the European Flood Alert System. *Hydrological Processes*, 25 (7), 1091–1113. doi:10.1002/hyp.7772

Pechlivanidis, I.G. and Arheimer, B., 2015. Large-scale hydrological modelling by using modified PUB recommendations: The India-HYPE case. *Hydrology and Earth System Sciences*, 19 (11), 4559–4579. doi:10.5194/hess-19-4559-2015

Pokorny, S., *et al.*, 2020. Use of ensemble-based gridded precipitation products for assessing input data uncertainty prior to hydrologic modeling. *Water*, 12 (10), 2751. doi:10.3390/w12102751

Prein, A.F. and Gobiet, A., 2017. Impacts of uncertainties in European gridded precipitation observations on regional climate analysis. *International Journal of Climatology*, 37 (1), 305–327. doi:10.1002/JOC.4706

Raimonet, M., *et al.*, 2017. Evaluation of gridded meteorological datasets for hydrological modeling. *Journal of Hydrometeorology*, 18 (11), 3027–3041. doi:10.1175/JHM-D-17-0018.1

Renard, B., *et al.*, 2010. Understanding predictive uncertainty in hydrologic modeling: the challenge of identifying input and structural errors. *Water Resources Research*, 46 (5), 5521. doi:10.1029/2009WR008328

Sarigil, G., Neri, M., and Toth, E., 2024. Evaluation of national and international gridded meteorological products for rainfall-runoff modelling in northern Italy. *Journal of Hydrology: Regional Studies*, 56, 102031. doi:10.1016/j.ejrh.2024.102031

Schreiner-McGraw, A.P. and Ajami, H., 2020. Impact of uncertainty in precipitation forcing data sets on the hydrologic budget of an integrated hydrologic model in mountainous terrain. *Water Resources Research*, 56 (12), e2020WR027639. doi:10.1029/2020WR027639

Schreiner-McGraw, A.P. and Ajami, H., 2022. Combined impacts of uncertainty in precipitation and air temperature on simulated mountain system recharge from an integrated hydrologic model. *Hydrology and Earth System Sciences*, 26 (4), 1145–1164. doi:10.5194/hess-26-1145-2022

Singh, V.P., 2018. Hydrologic modeling: progress and future directions. *Geoscience Letters*, 5 (1), 15. doi:10.1186/s40562-018-0113-z

Sperna Weiland, F.C., *et al.*, 2015. Significant uncertainty in global scale hydrological modeling from precipitation data errors. *Journal of Hydrology*, 529, 1095–1115. doi:10.1016/j.jhydrol.2015.08.061

Sun, Q., *et al.*, 2018. A review of global precipitation data sets: data sources, estimation, and intercomparisons. *Reviews of Geophysics*, 56 (1), 79–107. doi:10.1002/2017RG000574

Tang, G., *et al.*, 2023. The impact of meteorological forcing uncertainty on hydrological modeling: a global analysis of cryosphere basins. *Water Resources Research*, 59, e2022WR033767. doi:10.1029/2022WR033767

Tang, G., *et al.*, 2025. Uncertainty hotspots in global hydrologic modeling: The impact of precipitation and temperature forcings. *Bulletin of the American Meteorological Society*, 106 (1), E146–E166. doi:10.1175/BAMS-D-24-0007.1

Tang, G., Clark, M.P., and Papalexiou, S.M., 2022. Em-earth: the ensemble meteorological dataset for planet Earth. *Bulletin of the American Meteorological Society*, 103 (4), E996–E1018. doi:10.1175/BAMS-D-21-0106.1

Tapas, M.R., *et al.*, 2025. Evaluating combinations of rainfall datasets and optimization techniques for improved hydrological predictions using the SWAT+ model. *Journal of Hydrology: Regional Studies*, 57, 102134. doi:10.1016/J.EJRH.2024.102134

Tarek, M., Brissette, F.P., and Arsenault, R., 2020. Evaluation of the ERA5 reanalysis as a potential reference dataset for hydrological modelling over North America. *Hydrology and Earth System Sciences*, 24 (5), 2527–2544. doi:10.5194/HESS-24-2527-2020

Tran, T.-N.-D., *et al.*, 2023. Robustness of gridded precipitation products for Vietnam basins using the comprehensive assessment framework of rainfall. *Atmospheric Research*, 293, 106923. doi:10.1016/j.atmosres.2023.106923

Tran, T.-N.-D., *et al.*, 2024. Investigating the future flood and drought shifts in the transboundary Srepok River basin using CMIP6 projections. *IEEE Journal of Selected Topics in Applied Earth Observations and Remote Sensing*, 17, 1–16. doi:10.1109/JSTARS.2024.3380514

Tsering, K., *et al*., 2022. Verification of two hydrological models for real-time flood forecasting in the Hindu Kush Himalaya (HKH) region. *Natural Hazards*, 110 (3), 1821–1845. doi:10.1007/s11069-021-05014-y

van Kempen, G., van der Wiel, K., and Melsen, L.A., 2021. The impact of hydrological model structure on the simulation of extreme runoff events. *Natural Hazards and Earth System Sciences*, 21 (3), 961–976. doi:10.5194/nhess-21-961-2021

Vörösmarty, C.J., *et al*., 2015. Fresh water goes global. *Science*, 349 (6247), 478–479. doi:10.1126/science.aac6009

Vrugt, J.A., *et al*., 2003. A shuffled complex evolution Metropolis algorithm for optimization and uncertainty assessment of hydrologic model parameters. *Water Resources Research*, 39 (8), 1201. doi:10.1029/2002WR001642

Wanders, N. and Wada, Y., 2015. Human and climate impacts on the 21st century hydrological drought. *Journal of Hydrology*, 526, 208–220. doi:10.1016/j.jhydrol.2014.10.047

Yuan, X., Wood, E.F., and Ma, Z., 2015. A review on climate-model-based seasonal hydrologic forecasting: physical understanding and system development. *WIREs Water*, 2 (5), 523–536. doi:10.1002/wat2.1088